



Induction Heating Process

During the thixoforming process, it is very important to obtain a uniform temperature, which affects the uniformity of the solid fraction, throughout the billet. Consequently, a heating method that can provide a suitable temperature profile throughout the billet must be chosen. Other parameters that must be considered include heating time (in order to minimize the total processing time), the level of control, and temperature consistency. An optimal design of the induction coil has been identified that best meets these criteria. In a previous study, the theoretical optimal coil design was verified through the FEM simulation of the induction heating process by using a general purpose finite element analysis code, ANSYS. So, in this study, the suitability of the coil design was also demonstrated by conducting induction-heating experiments. The optimal reheating conditions to apply the thixoforming (thixoforging and semisolid die casting) process were investigated by varying the reheating time, the holding time, the reheating temperatures, the capacity of the induction heating system, and the size of the adiabatic material. The final holding time was observed to be the most important factor in obtaining a fine globular microstructure and to prevent coarsening in the three-step reheating process.

I. INTRODUCTION

FOR the thixoforming process, both the coexisting solidus-liquidus phase and the reheating conditions to obtain the globular microstructure are very important. In a study on the **induction heating process** of semisolid materials (SSM), Sebus and Henneberger^[1] verified that the design of the induction coil had an important influence on the induction heating process. Matsuura and Kitamura^[2] suggested that it is very important not to destroy the crystallization matrix of semisolid metals due to the change of the size of spherical dendrite grains during reheating. In a study on the induction heating of semisolid aluminum alloys, Midson *et al.*^[3] proposed that a coil design was necessary for uniform induction heating. Rudnev and co-workers^[4-7] showed that the required temperature distribution along the end of the slug depends on the frequency, the coil and slug geometry (including the slug-to-coil air gap and coil overhang), the material properties of the slug, its emissivity, coil refractory, power density, and cycle time. Hirt and co-workers^[8,9] and Garat and co-workers^[10-13] have both repeatedly emphasized that it is important to prevent the coarsening for thixoforming because, generally, an average grain size below 100 μm in the reheated state will be sufficient to ensure a homogeneous material flow of the semisolid alloy and good dimensional stability during die filling. Kang *et al.*^[14] experimentally proposed the optimal reheating conditions for thixoforging and the semisolid die casting processes using SSM (A356 alloys) with $d \ 3 \ 1 \ 5 \ 3 \ 9 \ 3 \ 8 \ 5 \ (\text{mm})$ and $d \ 3 \ 1 \ 5 \ 7 \ 6 \ 3 \ 6 \ (\text{mm})$. Jung and Kang^[15] proposed and manufactured an

the billet and to obtain a globular microstructure for thixoforging and semisolid die casting processes by using A356 (ALTHIX) alloy with $d \ 3 \ 1 \ 5 \ 7 \ 6 \ 3 \ 9 \ 0 \ (\text{mm})$ and a 60 Hz frequency for the induction heating system. Moreover, they demonstrated the suitability of the coil design by performing reheating experiments.

The effects of reheating time, billet size, and holding temperature on microstructures for the semisolid die casting and thixoforging of Al-6 Pct Si-3 Pct Cu-0.3 Pct Mg alloy (ALTHIX 86S) have not been reported. Therefore, the objective of this study is to determine the effects of the reheating conditions on the globularization of microstructures. The reheating time, the holding temperature, the holding time, the adiabatic material size, and the capacity of the induction heating system were considered as parameters of the globularization of microstructure. Particular interest is focused on the solutions avoiding the coarsening phenomena. Moreover, as the first part of our investigation, the optimal coil design to reduce the temperature gradient of the ALTHIX 86S billet and to obtain the globular microstructure was theoretically proposed and manufactured. The suitability of the coil design was demonstrated by using reheating experiments.

II. THE NECESSITY OF INDUCTION COIL DESIGN

During induction heating, the relationship between time and temperature must be controlled exactly to obtain a uniform temperature distribution over the entire cross-sectional area. Because the initial eutectic temperature (*i.e.*, initial solid fraction) in the thixoforming process is the key parameter to filling results in the thixoforming process, an accurately controllable induction heating method must be selected as the reheating process.

For the thixoforming process, the reheating of the billet in the semisolid state as quickly and homogeneously as possible is one of the most decisive aspects. From this point

of view, the design of the induction coil is very important. For a real system consisting of coil and billet, the induced heat over the length of the billet is normally not equally distributed, and consequently, there is a nonuniform temperature distribution. Therefore, an important point for the optimization of coil design is to verify the correct relationship between coil length and billet length.

In this study, the optimal coil design of the commercial induction heating system (for semisolid forming: 60 Hz) to obtain the globular microstructure for variations of SSM and specimen size (diameter and length) was theoretically proposed and manufactured. The suitability of the coil design will be demonstrated by using induction heating experiments.

III. COIL DESIGN FOR INDUCTION HEATING

For uniform reheating in this study, the optimal coil length, H , and a coil inner diameter, D_i , of the induction heating system were designed, as shown in Figure 1.

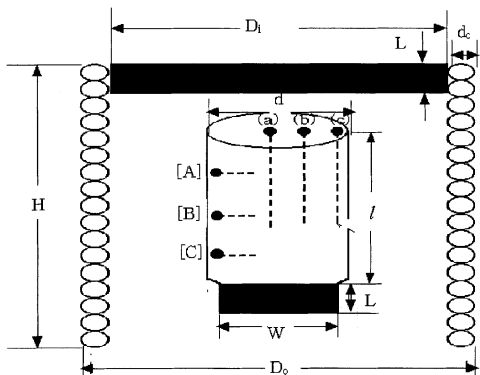
To consider the main surface power loss in induction heating, the idealized power density (P_s) must be represented as the actual power density (P_a), which is modified to allow for the ratio ($d/2d_F$) of a finite current depth of penetration (d_F) of material and billet diameter (d).

$$d_F \leq \frac{2r_a}{m \nu} \quad [1]$$

$$P_a \leq \frac{P_s (u_s \geq u_c)_{\text{idealized}}}{u_s \geq u_c} \leq \frac{6.89_K (u_s \geq u_c)}{d} \quad [2]$$

In Eq. [2], $\frac{u_s \geq u_c}{(u_s \geq u_c)_{\text{idealized}}} \leq k$ can be obtained from the variation curves of temperature in a cylinder with finite current depth of penetration.^[16]

In the preceding equation, r_a , m , ν , k , and $u_s \geq u_c$ are the resistivity of ALTHIX 86S, the magnetic constant, the angular frequency, the thermal conductivity, and the maximum surface-center temperature difference, respectively.



[A] [B] [C] : Thermocouple positions
(a) (b) (c) : "

D_o (mm)	D_i (mm)	d (mm)	H (mm)	l (mm)	d_c (mm)	L (mm)	W (mm)
120	100	76	180	70	10	19 or 20	53 or 50

Fig. 1—Schematic illustration of induction heating of cylindrical specimen.

If ALTHIX 86S with $d \leq 1576370$ (mm) is assumed to be 11 billets heating for a unit hour to 578 °C, the thermal capacity (Q) and the production rate (P_r) are calculated by Stansel's^[17] data (in the case of a temperature rise to 510 °C, the thermal capacity and the production rate are $Q \leq 145$ kW h/t and $P_r \leq 0.01$ t/h, respectively) and linear interpolation.

The minimum heated surface area (A_s) and the minimum heated length (l_w) can be determined as follows:

$$A_s \leq \frac{P_t}{P_a} \leq \frac{P_r \geq Q}{P_a} \quad [3]$$

$$l_w \leq \frac{A_s}{\pi d} \quad [4]$$

To determine the coil inner diameter D_i and optimal coil length H , recommended air gaps ($1/2 (D_i \geq d)$) for through-heating coils and property values to calculate the optimal coil length are shown in Tables I and II, respectively.

By using linear interpolation with Table I, the coil inner diameter D_i is calculated, and from the result of Eq. [4], the optimal coil length H is calculated as follows:

$$H \leq l_w \leq 1 (25 \text{ to } 75) \quad [5]$$

Therefore, from the preceding considerations, the coil dimensions for the SSM (ALTHIX 86S alloys) with $d \leq 1576370$ (mm) are proposed in Table III, and the experiments of induction heating are carried out using the designed dimensions.

We demonstrated the suitability of an optimal coil design through the finite element modeling simulation of the induction heating process by using a general purpose finite element analysis code, ANSYS.*^[20] In addition, the results of

*ANSYS is a trademark of Swanson Analysis Systems, Inc., Houston, PA.

induction heating CAE based on the optimal coil design for variations of SSM and specimen size coincided with those of the induction heating experiment.^[20,21]

IV. INDUCTION HEATING EXPERIMENTS

For the thixoforming process, the billet must be reheated to a semisolid state. The induction heating process is very important in the forming process of an SSM billet, the process not only being necessary to achieve the required SSM billet state, but also to control the microstructure of the billet.

The SSM used in this study was an ALTHIX 86S alloy fabricated by electromagnetic stirring by PECHINEY in France. This SSM is a casting alloy used in the development of automotive parts. The chemical composition is shown in Table IV, and the microstructure of the raw material is shown in Figure 2.

The ALTHIX 86S alloy is machined to $d \leq 1576370$

Table I. Recommended Air Gaps [$1/2 (D_i \geq d)$] for Through-Heating Coils^[16]

Frequency	Billet Temperature (°C)	Billet Diameter (d , mm)		
		0 to 60	60 to 125	125 to 250
50/60 Hz	550	12	12	12
	850	12	20	40

Table II. Property Values to Calculate the Optimal Coil Length (Specimen Size: $d \ 3 \ 1 \ 5 \ 76 \ 3 \ 70 \text{ mm}$, $f \ 5 \ 60 \text{ Hz}$, and $k \ 5 \ 0.58$)

Parameters	Symbol	Unit	Values	Reference
Maximum surface-center temperature difference	$u_s \ 2 \ u_c$	K mm	4	—
Current depth of penetration	d	W/m K	10.7	18
Thermal conductivity	k	kW/m ²	109	19
Idealized power density	P_s	mV/m	22.91	—
Resistivity of ALTHIX 86S	r_a	H/m	0.0639	19
Magnetic constant	m	rad/s	$4\pi \ 3 \ 10^{27}$	16
Angular frequency	ν	m	120p	—
Finite current depth of penetration	d_F	kW/m ²	$1.64 \ 3 \ 10^{22}$	—
Actual power density	P_a	kW	39.5	—
Thermal power	P_t	dimensionless	1.33	—
Production rate	P_r	kW	0.01 t/h	17
Thermal capacity	Q	m ²	133.08 h/t	—
Minimum heated surface area	A_s	mm	$30.67 \ 3 \ 10^{23}$	—
Billet diameter	d	mm	76	—
Minimum heated length	l_w		141	—

Table III. Designed Dimensions of Induction Heating Device ($f \ 5 \ 60 \text{ Hz}$, $d \ 5 \ 10.7 \text{ mm}$,^[18] $l \ 5 \ 70 \text{ mm}$, and $k \ 5 \ 0.58$)

Billet Diameter (d , mm)	Coil Inner Diameter (D_i , mm)	Minimum Heating Length (l_w , mm)	Optimal Coil Length (H , mm)
76	100	141	166 to 216

Table IV. Chemical Compositions of ALTHIX 86S

	Si	Fe	Cu	Mn	Mg	Cr	Zn	Ti	Pb
Minimum (pct)	5.5	—	2.5	—	0.30	—	—	—	—
Maximum (pct)	6.5	0.15	3.5	0.03	0.40	—	0.05	0.20	0.03

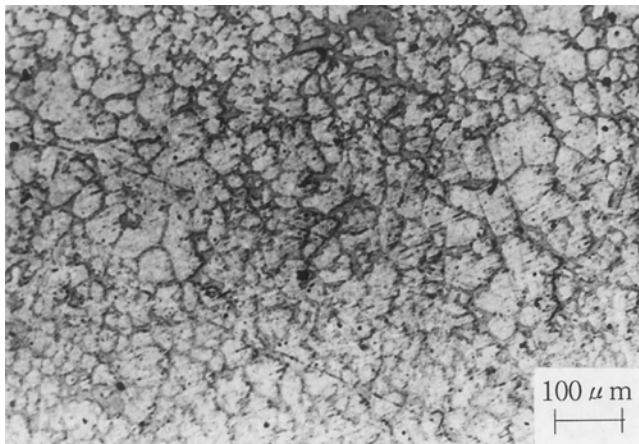


Fig. 2—Microstructure for raw material of ALTHIX 86S.

(mm). The experiments of induction heating were performed by using an induction heating system (frequency: 60 Hz) with the capacity of 50 kW. As shown in Figure 1, to achieve uniform heating, the heating coil of the induction heating system is made by machining to $D_0 \ 3 \ H \ 5 \ 120 \ 3 \ 180$

(mm).^[20,21] Thermocouple holes (2-mm diameter) to measure the temperature are accurately machined at 45 mm from the surface of the billet and at 10 mm from the lateral of the billet. To accurately control the temperature of the SSM, K-type CA thermocouples (sheath type) of $w \ 1.6 \text{ mm}$ are inserted into the billet. Thermocouples are calibrated by means of being inserted into water of 100 °C. The accuracy of thermocouples is approximately 0.2 pct. Data logger TDS-302 (Tokyo Sokki Kenkyuio Co., Ltd.) was used to receive the data, and the heating temperature was set to the datum at thermocouple position (b) in Figure 1.

To determine the optimal reheating conditions, the following parameters were used for the globularization of the microstructure and a small temperature gradient: the capacity of the induction heating system (Q), the reheating time (t_a), the holding temperature (T_h), the holding time (t_h), the reheating step, and the adiabatic material size. The reheating experiments were performed under the conditions in Table V. The meanings of the symbols used in Table V are the same as those shown in Figure 3.

V. THE RESULTS OF INDUCTION HEATING AND DISCUSSION

After [induction heating](#), the microstructure of the SSM must be globular. Moreover, when the SSM is fed from the induction heating system to the die, the shape of the SSM must be maintained. Therefore, the capacity of the induction heating system (Q), the reheating time (t_a), the holding temperature (T_h), the holding time (t_h), the reheating step, and the adiabatic material size were considered as parameters of the experiment to observe the globularization of the microstructure and a small temperature gradient.

The relationship between temperature and solid fraction of the ALTHIX 86S alloy is given in Figure 4. The temperatures corresponding to the solid fractions of 50 and 55 pct are 582 °C and 578 °C, respectively.^[10] Generally, these solid fractions of 50 and 55 pct are for semisolid die casting and thixoforging, respectively.

VI. SOLID FRACTION 55 PCT

Reheating experiments 1 through 19 were performed for $f_s \ 5 \ 55 \text{ pct}$. From experiments 1 through 10, the experiments

Table V. Experimental Conditions for Reheating of Semisolid Aluminum Alloy (ALTHIX 86S), Test Specimen Size:
***d* 3 1 5 76 3 70 (mm)**

Number	Reheating Time t_a (min)			Holding Temperature T_h (°C)			Holding Time t_h (min)			Total Time (min)	Capacity Q (kW)	Adiabatic Material Size (mm) $D \ 3 \ W \ 3 \ L$
	t_{a1}	t_{a2}	t_{a3}	T_{h1}	T_{h2}	T_{h3}	t_{h1}	t_{h2}	t_{h3}			
1	4	3	1	350	567	578	1	3	2	14	8.398	without
2	4	3	1	350	567	578	1	3	2	14	7.480	without
3	4	3	1	350	567	578	1	3	2	14	5.945	without
4	4	3	1	350	567	578	1	3	2	14	3.912	without
5	4	3	1	350	567	578	1	3	2	14	4.096	without
6	4	3	1	350	567	578	1	3	2	14	4.941	without
7	4	3	1	350	567	578	1	3	2	14	5.292	without
8	4	3	1	350	567	578	1	3	2	14	5.544	without
9	4	3	1	350	567	578	1	3	2	14	5.482	without
10	4	3	1	350	567	578	1	3	2	—	5.012	without
11	10	—	—	578	—	—	2	—	—	12	5.544	50 3 50 3 20
12	12	—	—	578	—	—	2	—	—	14	5.544	50 3 50 3 20
13	8	1	—	567	578	—	3	2	—	14	5.544	50 3 50 3 20
14	8	2	—	567	578	—	1	2	—	15	5.544	50 3 50 3 20
15	4	3	1	350	567	578	1	3	1	13	5.544	50 3 50 3 20
16	4	3	1	350	567	578	1	3	2	14	5.544	50 3 50 3 20
17	4	3	1	350	567	578	1	3	3	15	5.544	50 3 50 3 20
18	4	3	2	350	567	578	1	3	2	15	5.544	50 3 50 3 20
19	4	4	2	350	567	578	1	3	2	16	5.544	50 3 50 3 20
20	4	3	1	350	572	582	1	3	2	14	5.544	50 3 50 3 20
21	4	3	1	350	572	582	1	3	2	14	5.231	50 3 50 3 20
22	4	3	1	350	567	582	1	3	2	14	4.941	50 3 50 3 20
23	4	3	1	350	567	582	1	3	2	14	4.806	50 3 50 3 20
24	4	3	1	350	567	582	1	3	2	14	5.376	50 3 50 3 20
25	4	3	1	350	567	582	1	3	2	14	5.448	50 3 50 3 20
26	4	3	1	350	567	582	1	3	2	14	5.128	53 3 53 3 19
27	4	3	1	350	567	582	1	3	4	16	5.128	53 3 53 3 19
28	4	3	1	350	567	582	1	3	3	15	5.128	53 3 53 3 19

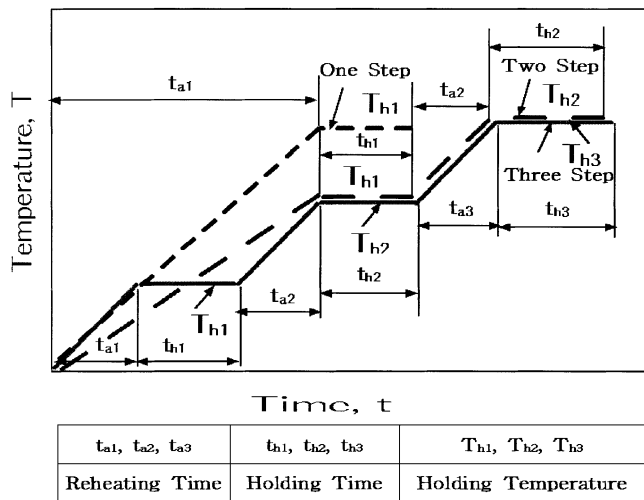


Fig. 3—Input data diagram of reheating conditions to obtain the globular microstructure.

were carried out at the reheating conditions of $t_{a1} \leq 4$ min, $t_{a2} \leq 3$ min, $t_{a3} \leq 1$ min, $t_{h1} \leq 1$ min, $t_{h2} \leq 3$ min, $t_{h3} \leq 2$ min, $T_{h1} \leq 350$ °C, $T_{h2} \leq 567$ °C, and $T_{h3} \leq 578$ °C, with a changing capacity of induction heating system to determine the optimal capacity according to the heating time. In the case of the capacity (Q) of 5.544 kW, the billets reach the set temperature with a small temperature difference.

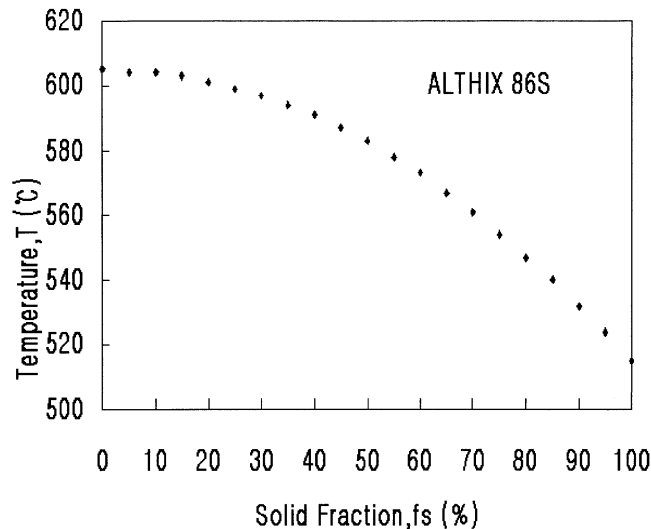


Fig. 4—Relationships between temperature and solid fraction for ALTHIX 86S.

Therefore, experiments 11 and 12 were performed at one-step heating conditions of $t_{h1} \leq 2$ min and $T_{h1} \leq 578$ °C, with the capacity (Q) of 5.544 kW. For experiments 11 and 12, when the size of adiabatic materials is $D \ 3 \ W \ 3 \ L \ 5 \ 50 \ 3 \ 50 \ 3 \ 20$ (mm), t_{a1} is 10 and 12 minutes, respectively. Figure 5 shows the microstructure of the reheated SSM for

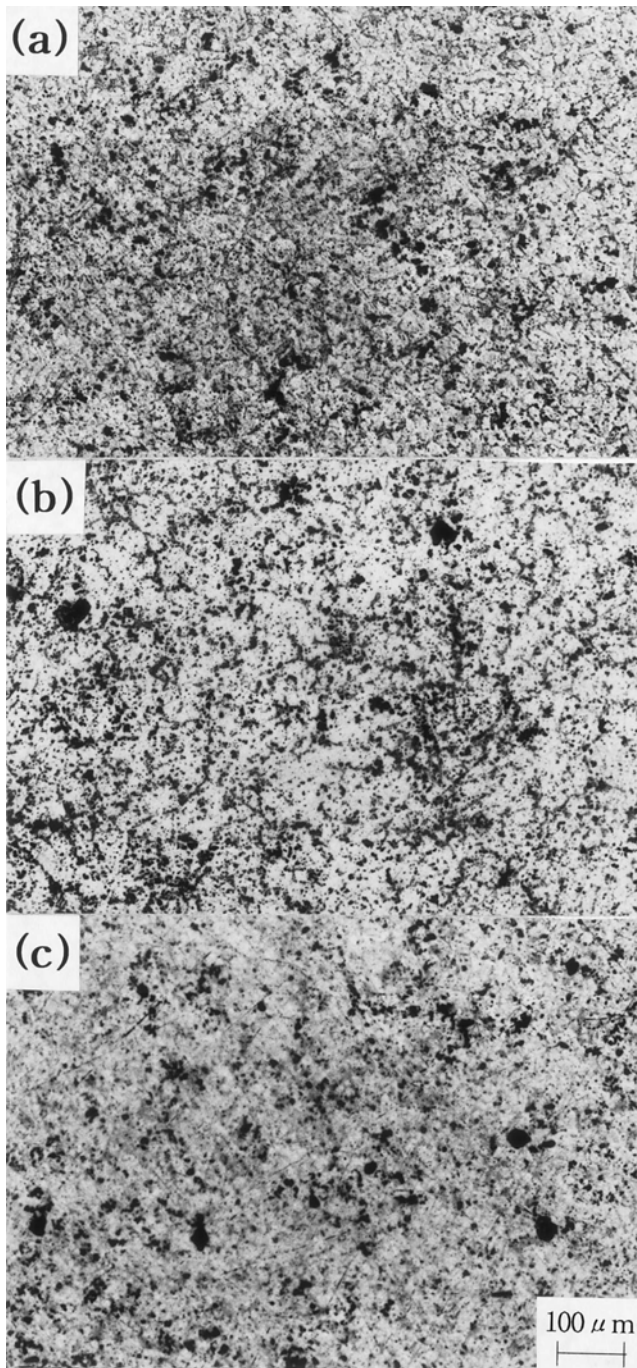


Fig. 5—(a) through (c) Microstructure in one-step reheating process of semisolid aluminum alloy (experiment 12, 86S, $f_s \leq 55$ pct, $t_{a1} \leq 12$ min, $T_{h1} \leq 578$ °C, $t_{h1} \leq 2$ min, and $Q \leq 5.544$ kW).

experiment 12. The globular microstructure was not obtained at positions (a), (b), and (c) of Figure 1. Due to the lack of sufficient holding time for the separation between solid and liquid before and after phase change and for globularization of a small Si primary crystal, one-step reheating is unsuitable for ALTHIX 86S with $d \leq 1 \leq 76 \leq 70$ (mm).

Experiments 13 and 14 were performed at two-step heating conditions of $t_{a1} \leq 8$ min, $t_{h1} \leq 3$ min, $t_{h2} \leq 2$ min, $T_{h1} \leq 567$ °C, $T_{h2} \leq 578$ °C, and $Q \leq 5.544$ kW. Moreover, when the size of the adiabatic material is $D \leq W \leq L \leq 50 \leq 30 \leq 30 \leq 20$ (mm), t_{a2} (t_{a2} is the time to reach T_{h2}) is 1 and

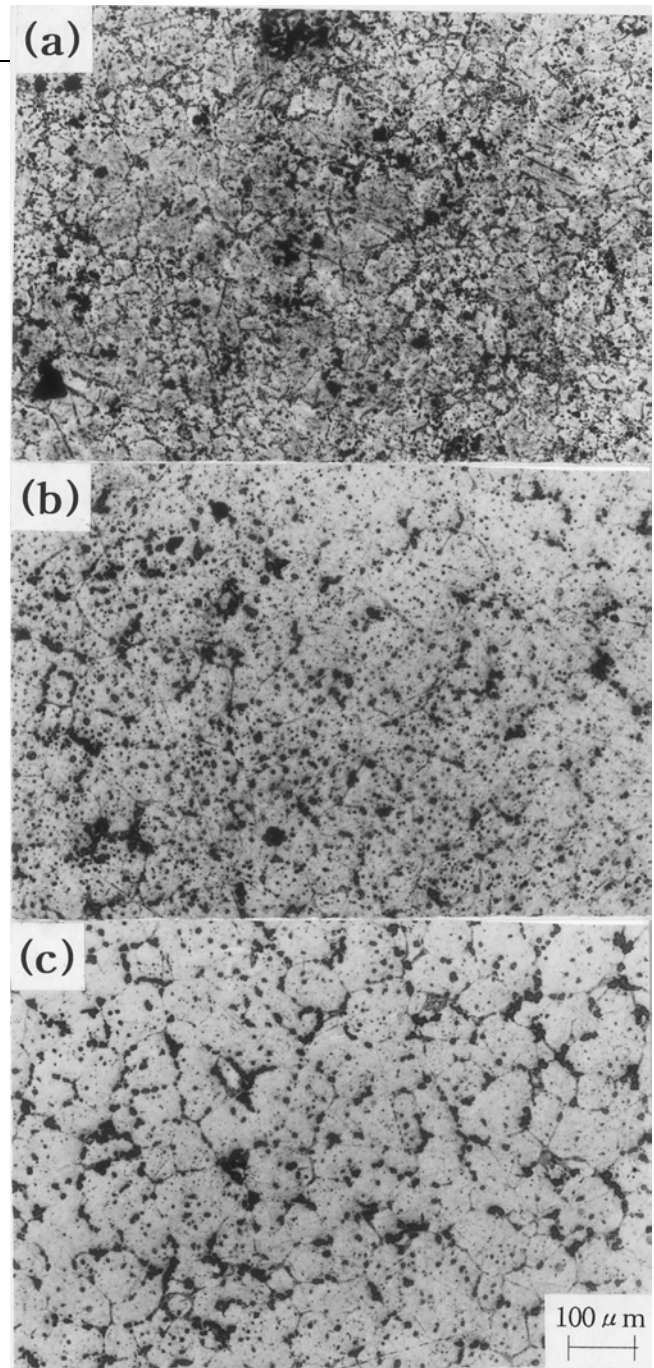


Fig. 6—(a) through (c) Microstructure in two-step reheating process of semisolid aluminum alloy (experiment 14, 86S, $f_s \leq 55$ pct, $t_{a1} \leq 8$ min, $t_{a2} \leq 2$ min, $T_{h1} \leq 567$ °C, $T_{h2} \leq 578$ °C, $t_{h1} \leq 3$ min, $t_{h2} \leq 2$ min, $Q \leq 5.544$ kW).

2 minutes, respectively. Figure 6 shows the microstructure of reheated SSM for experiment 14 of Table V. The temperature difference of the reheated SSM at the measuring positions is 62 °C. The microstructure of Figure 6 is not globular at positions (a) and (b) of Figure 1, and the globularization is in progress at the position (c). Due to the lack of sufficient holding time for the separation between solid and liquid before and after phase change, and for globularization of a small Si primary crystal, two-step reheating is also unsuitable for ALTHIX 86S with $d \leq 1 \leq 76 \leq 70$ (mm).

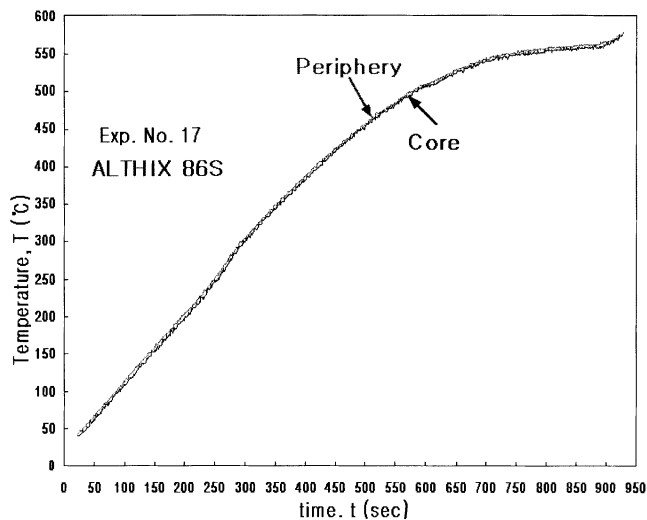


Fig. 7—Temperature distributions in three-step reheating process of semi-solid alloy ($f_s \leq 55$ pct, $t_{a1} \leq 4$ min, $t_{a2} \leq 3$ min, $t_{a3} \leq 1$ min, $T_{h1} \leq 350$ °C, $T_{h2} \leq 567$ °C, $T_{h3} \leq 578$ °C, $t_{h1} \leq 1$ min, $t_{h2} \leq 3$ min, $t_{h3} \leq 3$ min, and $Q \leq 5.544$ kW).

Experiments 15 through 17 of Table V were performed at three-step heating conditions of $t_{a1} \leq 4$ min, $t_{a2} \leq 3$ min, $t_{a3} \leq 1$ min, $t_{h1} \leq 1$ min, $t_{h2} \leq 3$ min, $T_{h1} \leq 350$ °C, $T_{h2} \leq 567$ °C, $T_{h3} \leq 578$ °C, and the capacity of $Q \leq 5.544$

kW. Moreover, when the size of the adiabatic material is $D \leq 3$ W 3 L 5 50 3 50 3 20 (mm), t_{h3} (t_{h3} is the time to reach T_{h3}) is 1, 2, and 3 minutes, respectively. In the case of experiment 17, which obtained the finest globular microstructure as shown in Figure 7, the temperature difference of the reheated SSM at the measuring positions is small. Figure 8 shows the microstructure of reheated SSM for experiments 15 through 17. In the case of experiment 15, globularization was in progress at the thermocouple position (a) of Figure 1, and a fine globular microstructure was observed at positions (b) and (c).

In the cases of experiments 16 and 17, a fine globular microstructure was obtained at positions (a) through (c) of Figure 1. Comparing experiments 15 through 17, the final reheating holding time (t_{h3}) is 1, 2, and 3 minutes, respectively, and the temperature difference of reheated SSM at the measuring positions is small. The microstructure of experiment 15 (performed at the condition of $t_{h3} \leq 1$ min) is not globular at position (a) of Figure 1. In the case of experiment 16 performed at the condition of $t_{h3} \leq 2$ min, the globular microstructure was obtained at positions (a) through (c) of Figure 1, but the degree of the globularization was not improved. The microstructure of experiment 17 (performed at the condition of $t_{h3} \leq 3$ min) is finer and more globular than that of experiment 16 (performed at the condition of $t_{h3} \leq 2$ min). Due to the lack of sufficient holding time to obtain a fine globular microstructure by the separation between agglomerated solid before and

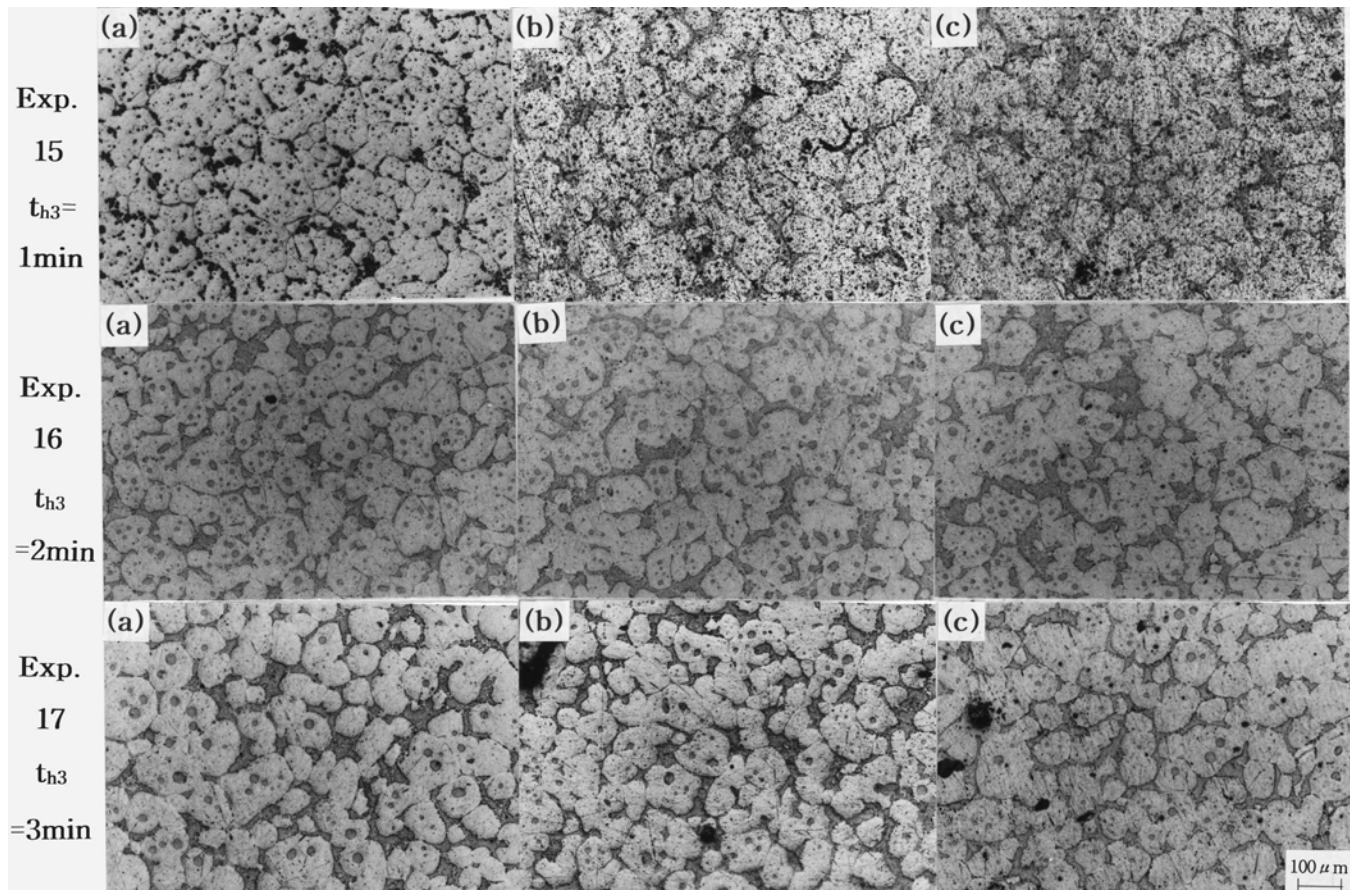


Fig. 8—(a) through (c) Microstructure in three-step reheating process of semisolid aluminum alloy (86S, $f_s \leq 55$ pct, $t_{a1} \leq 4$ min, $t_{a2} \leq 3$ min, $t_{a3} \leq 1$ min, $T_{h1} \leq 350$ °C, $T_{h2} \leq 567$ °C, $T_{h3} \leq 578$ °C, $t_{h1} \leq 1$ min, $t_{h2} \leq 3$ min, and $Q \leq 5.544$ kW).

after phase change, the reheating conditions of experiment 16 are unsuitable.

Experiments 18 and 19 of Table V were performed at the conditions of $t_{a1} \leq 4$ min, $t_{a3} \leq 2$ min, $t_{h1} \leq 1$ min, $t_{h2} \leq 3$ min, $t_{h3} \leq 2$ min, $T_{h1} \leq 350$ °C, $T_{h2} \leq 567$ °C, $T_{h3} \leq 578$ °C, and the capacity of $Q \leq 5.544$ kW. Moreover, when the size of the adiabatic material is $D \ 3 \ W \ 3 \ L \ 50 \ 3 \ 50 \ 3 \ 20$ (mm), t_{a2} is 3 and 4 minutes, respectively. Figure 9 shows the microstructure of reheated SSM for experiment 18. The temperature difference of reheated SSM at the measuring

positions is small, and in the case of experiment 18, the globular microstructure is obtained at positions (a) through (c) in Figure 1.

Compared to experiment 17, which obtained a fine globular microstructure, in the case of experiment 18, the temperature difference of reheated SSM at the measuring positions is larger. Experiment 18 shows good globularization, but shows cohesion between solid regions at positions (a) through (c) of Figure 1.

VII. SOLID FRACTION 50 PCT

Reheating experiments 20 through 28 were performed for $f_s \leq 50$ pct. From experiments 20 through 26 of Table V, the experiments are carried out at the reheating conditions of $t_{a1} \leq 4$ min, $t_{a2} \leq 3$ min, $t_{a3} \leq 1$ min, $t_{h1} \leq 1$ min, $t_{h2} \leq 3$ min, $t_{h3} \leq 2$ min, $T_{h1} \leq 350$ °C, $T_{h2} \leq 572$ °C, and $T_{h3} \leq 582$ °C, changing the capacity of the induction heating system to determine the optimal capacity according to the heating time. The sizes of adiabatic materials are $D \ 3 \ W \ 3 \ L \ 50 \ 3 \ 50 \ 3 \ 20$ (mm) from experiments 20 through 25, and $D \ 3 \ W \ 3 \ L \ 53 \ 3 \ 53 \ 3 \ 19$ (mm) for experiment 26, respectively. In the case of $Q \leq 5.128$ kW, the billet reaches the set temperature with a temperature difference of 62 °C.

The reheating experiments of experiments 27 and 28 of Table V were performed under the reheating conditions of experiment 26 with $t_{h3} \leq 4$ min and $t_{h3} \leq 3$ min (t_{h3} is the final holding time in a three-step reheating), respectively. Figures 10 and 11 show the temperature distribution and microstructure of reheated SSM for experiment 28 of Table V. The temperature difference of reheated SSM at the measuring positions is small, and in the case of experiment 27, the globular microstructure was coarse at positions (a) through and (c) of Figure 1. However, in the case of experiment 28, a fine globular microstructure was obtained at positions (a) through (c). Compared to experiment 28, the microstructure of experiment 27 becomes coarse by the

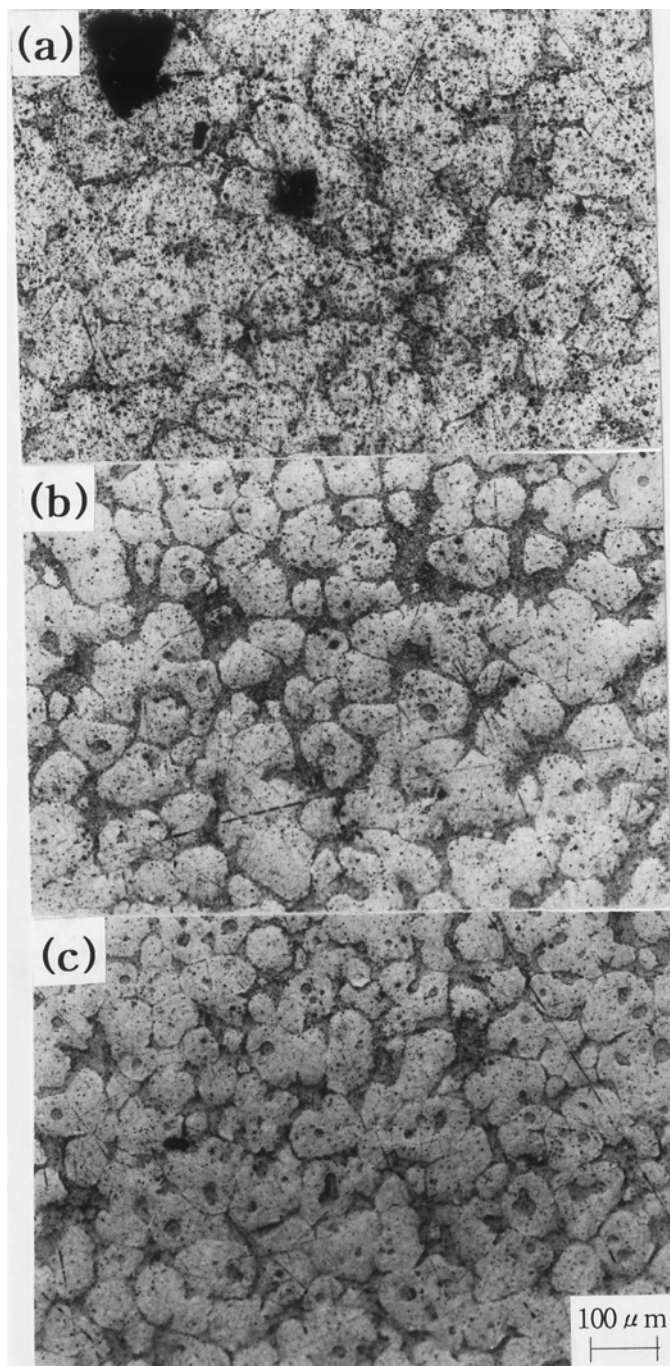


Fig. 9—(a) through (c) Microstructure in three-step reheating process of semisolid aluminum alloy (experiment 18, 86S, $f_s \leq 55$ pct, $t_{a1} \leq 4$ min, $t_{a2} \leq 3$ min, $t_{a3} \leq 2$ min, $T_{h1} \leq 350$ °C, $T_{h2} \leq 567$ °C, $T_{h3} \leq 578$ °C, $t_{h1} \leq 1$ min, $t_{h2} \leq 3$ min, $t_{h3} \leq 2$ min, and $Q \leq 5.544$ kW).

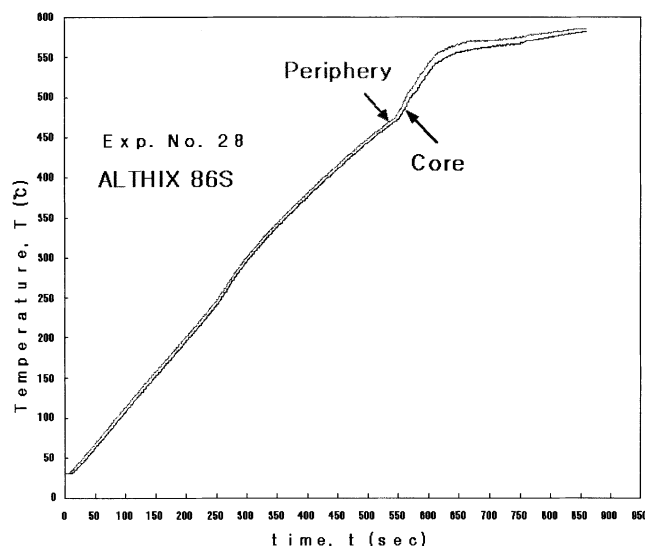
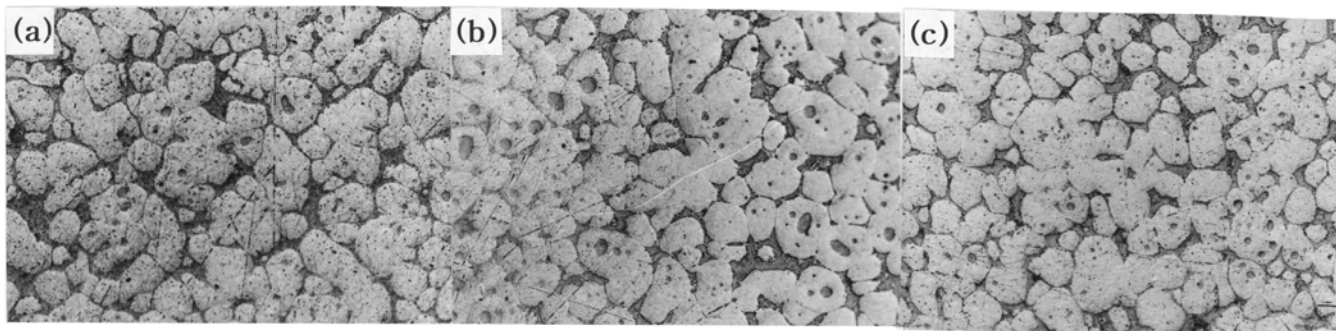
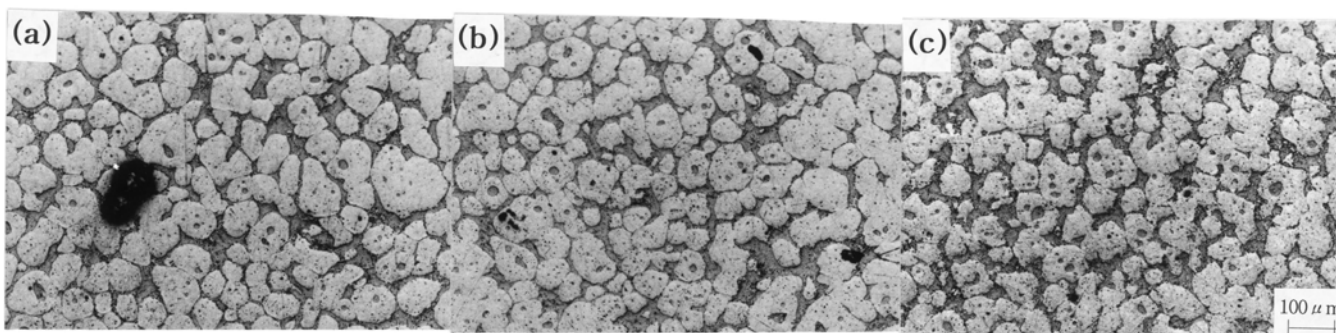


Fig. 10—Temperature distributions in three-step reheating process of semisolid aluminum alloy ($f_s \leq 50$ pct, $t_{a1} \leq 4$ min, $t_{a2} \leq 3$ min, $t_{a3} \leq 1$ min, $T_{h1} \leq 350$ °C, $T_{h2} \leq 572$ °C, $T_{h3} \leq 582$ °C, $t_{h1} \leq 1$ min, $t_{h2} \leq 3$ min, $t_{h3} \leq 3$ min, and $Q \leq 5.544$ kW).



(a) Exp. No. 27, $t_{h3}=2\text{min}$



(b) Exp. No. 28, $t_{h3}=3\text{min}$

Fig. 11—(a) through (c) Microstructure in three-step reheating process of semisolid aluminum alloy (86S, $f_s \leq 50$ pct, $t_{a1} \leq 4$ min, $t_{a2} \leq 3$ min, $t_{a3} \leq 1$ min, $T_{h1} \leq 350$ °C, $T_{h2} \leq 572$ °C, $T_{h3} \leq 582$ °C, $t_{h1} \leq 1$ min, $t_{h2} \leq 3$ min, and $Q \leq 5.128$ kW).

growth and coalescence due to longer holding time than that of experiment 28.

VIII. COMPARISON BETWEEN SOLID FRACTION 50 AND 55 PCT

Through reheating experiments for $f_s \leq 50$ and 55 pct, it was found that the higher the solid fraction, the worse the accuracy of globularization, but the boundary between the solid regions and the liquid regions is clear.

Figure 12 shows the micrographs magnified to the scale of 1000 to observe the eutectic microstructure of experiments 17 and 28, which obtained the finest globular microstructure for $f_s \leq 55$ and 50 pct. Figures 12(a) and (b) show that the eutectic is melted completely. Therefore, it was found that the eutectic must be melted completely at over 572 °C (complete eutectic melting temperature of ALTHIX 86S alloy), and the reheating time for the complete eutectic melting is necessary to obtain a fine globular microstructure. The rise in temperature does not occur until a sufficient amount of thermal energy to melt the eutectic is provided because so much thermal energy and time are necessary to melt the eutectic.^[14,15] Before and after the melting of the eutectic, the solid fraction changes rapidly, and a rapid temperature rise occurs when the eutectic is melted. Due to this temperature rise, controlling the reheating temperature is difficult. Therefore, to homogeneously control the temperature distribution and the solid fraction of the SSM, the billet must be reheated in three steps.

It was found that in the case of the ALTHIX 86S alloy with $d \leq 315$ mm (Figure 5), one-step reheating

is not a good condition because the size of the solid grain is small, but the globularization of the microstructure is not obtained. As shown in Figure 6, two-step reheating also is not relevant due to the lack of sufficient holding time to allow for the separation between solid and liquid before and after phase change and for globularization of a small Si particle.

The holding time of the final step is very important in the three-step reheating process. As shown in Figures 8(a) and (b), if the holding time of the final step is short, the microstructure of the globularization is not obtained or not accurate due to the lack of sufficient holding time for the separation between a solid and a liquid, before and after phase change, and for globularization by the growth of a small Si primary crystal. On the other hand, if the holding time of the final step is too long, the microstructure becomes coarse due to the growth and coalescence of solid regions rather than the refining of globular Si primary crystal,^[22] as shown in Figure 11(a). Therefore, the optimal holding time of the final step to obtain a fine globular microstructure without agglomeration is 3 minutes.

Figure 13 shows the optimal reheating conditions to obtain a fine globular microstructure that is available for thixoforming according to the alloys and specimen sizes. Compared to the reheating conditions performed by using A356 alloys with $d \leq 315$ mm (39.3 mm) and $d \leq 315$ mm (76.3 mm) by Kang *et al.*^[14] by whom the finest globular microstructure is obtained in one-step reheating conditions ($t_{a1} \leq 10$ min, $t_{h1} \leq 2$ min, $T_{h1} \leq 573$ °C, $Q \leq 3.3$ kW) for $d \leq 315$ mm (39.3 mm) and in two-step reheating conditions ($t_{a1} \leq 8$ min,

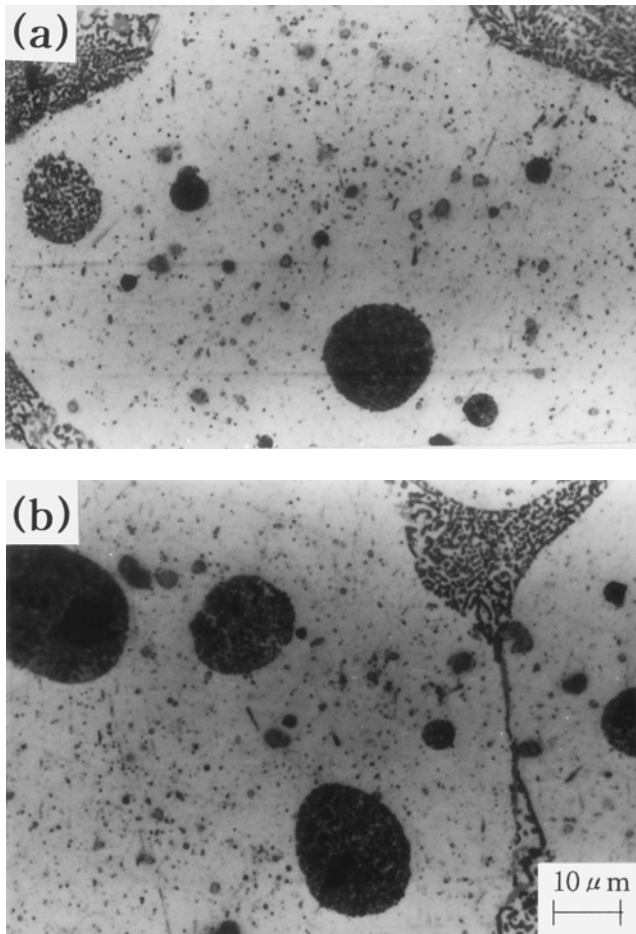


Fig. 12—(a) Exp. No. 17, $f_s \leq 55$ pct, $t_{a1} \leq 4$ min, $t_{a2} \leq 3$ min, $t_{a3} \leq 1$ min, $T_{h1} \leq 350$ °C, $T_{h2} \leq 567$ °C, $T_{h3} \leq 578$ °C, $t_{h1} \leq 1$ min, $t_{h2} \leq 3$ min, $t_{h3} \leq 3$ min, $Q \leq 5.544$ kW and (b) Exp. No. 28, $f_s \leq 50$ pct, $t_{a1} \leq 4$ min, $t_{a2} \leq 3$ min, $t_{a3} \leq 1$ min, $T_{h1} \leq 350$ °C, $T_{h2} \leq 572$ °C, $T_{h3} \leq 582$ °C, $t_{h1} \leq 1$ min, $t_{h2} \leq 3$ min, $t_{h3} \leq 3$ min, $Q \leq 5.128$ kW. Eutectic microstructure of semisolid alloy (ALTHIX 86S).

$t_{a2} \leq 1$ min, $t_{h1} \leq 3$ min, $t_{h2} \leq 2$ min, $T_{h1} \leq 575$ °C, $T_{h2} \leq 584$ °C, $Q \leq 3.00$ kW) for $d \leq 1 \leq 76 \leq 60$ (mm).

According to reported results using A356 alloys with $d \leq 3 \leq 76 \leq 90$ (mm) by Jung and co-workers,^[15,21] the

finest globular microstructure is obtained in three-step conditions ($t_{a1} \leq 4$ min, $t_{a2} \leq 3$ min, $t_{a3} \leq 1$ min, $t_{h1} \leq 1$ min, $t_{h2} \leq 3$ min, $t_{h3} \leq 2$ min, $T_{h1} \leq 350$ °C, $T_{h2} \leq 575$ °C, $T_{h3} \leq 584$ °C, $Q \leq 8.398$ kW, and the size of the adiabatic material is $D \leq 3 \leq 53 \leq 53 \leq 19$ (mm)) for $f_s \leq 50$ pct and in three-step conditions ($t_{a1} \leq 4$ min, $t_{a2} \leq 3$ min, $t_{a3} \leq 1$ min, $t_{h1} \leq 1$ min, $t_{h2} \leq 3$ min, $t_{h3} \leq 2$ min, $T_{h1} \leq 350$ °C, $T_{h2} \leq 570$ °C, $T_{h3} \leq 576$ °C, $Q \leq 12.04$ kW, and the size of the adiabatic material is $D \leq 3 \leq 50 \leq 50 \leq 20$ (mm)) for the solid fraction of $f_s \leq 55$ pct.

In this study using ALTHIX 86S alloys with $d \leq 3 \leq 76 \leq 70$ (mm), the finest globular microstructure was obtained in three-step conditions ($t_{a1} \leq 4$ min, $t_{a2} \leq 3$ min, $t_{a3} \leq 1$ min, $t_{h1} \leq 1$ min, $t_{h2} \leq 3$ min, $t_{h3} \leq 3$ min, $T_{h1} \leq 350$ °C, $T_{h2} \leq 567$ °C, $T_{h3} \leq 578$ °C, $Q \leq 5.544$ kW, and the size of the adiabatic material was $D \leq 3 \leq 50 \leq 50 \leq 20$ (mm)) for $f_s \leq 55$ pct and in three-step conditions ($t_{a1} \leq 4$ min, $t_{a2} \leq 3$ min, $t_{a3} \leq 1$ min, $t_{h1} \leq 1$ min, $t_{h2} \leq 3$ min, $t_{h3} \leq 3$ min, $T_{h1} \leq 350$ °C, $T_{h2} \leq 572$ °C, $T_{h3} \leq 582$ °C, $Q \leq 5.128$ kW, and the size of the adiabatic material was $D \leq 3 \leq 53 \leq 53 \leq 19$ (mm)) for the solid fraction of $f_s \leq 50$ pct.

IX. GRAIN GROWTH MECHANISM OF ALTHIX 86S ALLOY

In the case of eutectic Al-Si alloys, mechanical properties such as wear resistance, strength, hardness, flowability at high temperature, and corrosion resistance are excellent due to the microstructure distributed with Si primary crystals inside the eutectic matrix. However, a coexisting solidus-liquidus interval increases with silicon content, and the microstructure becomes coarse when a strong electromagnetic stirring force occurs.

Therefore, it is important to prevent the coarsening (over 100 μm) of Si primary crystals for thixoforming, because, generally, an average grain size below 100 μm in the reheated state will be sufficient to ensure a homogeneous material flow of the semisolid alloy and good dimensional stability during die filling.^[9–13,21]

The factor commonly used to explain the coarsening phenomena of the primary particles is the orientation relationship between particles. The experiments were performed by changing the reheating conditions such as solid fraction,

Alloys	Billet Size d× l(mm)	Optimal Reheating Conditions										Step	Ref.
		t _a (min)			t _h (min)		T _h (°C)		Q (KW)				
		t _{a1}	t _{a2}	t _{a3}	t _{h1}	t _{h2}	t _{h3}	T _{h1}	T _{h2}	T _{h3}			
A356	39×85	10			2			573			3.3	1	[14]
	60×90	4	4	1	1	2	1	350	565	576	12.5	3	[20]
	76×60	8	1		3	2		570	576		3.0	2	[14]
	76×90	4	3	1	1	3	2	350	570	576	12.04	3	[15, 21]
Al2024	60×90	4	3	1	1	3	1	350	603	616	8.6	3	[20]
ALTHIX 86S	76×70	4	3	1	1	3	3	350	567	578	5.544	3	

Fig. 13—Input data diagram of optimal reheating conditions to obtain the globular microstructure for variation of alloys and specimen size.

heating time, and reheating holding time. However, no change of the orientation relationship between particles was detected through experiments.

It is seen that the bonding between particles in the reheating process does not occur along certain crystallographic directions but occurs in disordered directions, and the globularized particles are coarse due to the coalescence between particles. Therefore, to prevent the coarsening of the particles, it is important to hold a relevant temperature for a constant time during each step, and in the case of three-step reheating, it is especially important in the final step. Induction heating of an aluminum billet over a diameter of 30 mm is effective at low frequencies. However, in the case of low frequencies, if the holding time at high temperatures is long, coarsening occurs through Ostwald growth, coalescence, and separation processes due to a strong electromagnetic stirring force.^[21,23]

In order to prevent the A356 alloy with $d\ 3\ 1\ 5\ 76\ 3\ 90$ (mm) from coarsening during reheating, it should be held for 2 minutes at 576 °C, and in the case of three-step reheating, that is the holding time during the final step.^[15] A356 and Al2024 alloys with $d\ 3\ 1\ 5\ 60\ 3\ 90$ (mm) are held for 1 minute at 576 °C and 616 °C, respectively.^[20,24] In this study, the ALTHIX 86S alloy with $d\ 3\ 1\ 5\ 76\ 3\ 70$ (mm) was used and held for 3 minutes at 578 °C.

Silicon primary crystals are simultaneously destroyed and coalesced by collisions between themselves, resulting in polycrystals with low- and high-angle boundaries. Furthermore, after the fracture and coalescence processes progress, the interface of Si primary crystals are gradually rounded by their collisions.^[21,25] The fracture, coalescence, and wear of Si primary particles occur compositively, and the initial facet Si particle is globularized at the end of induction heating.

Research on the globularization phenomena beside a coexisting solidus-liquidus interval has focused mainly on alloys with a nonfaceted interface. In the case of the Al2024 alloy with a nonfaceted interface, the interfacial energy between solid and liquid does not change for the variation of crystallographic directions.^[21,26]

However, in the ALTHIX 86S alloy with a faceted interface, the flat interface is a simple cubic crystal surrounded by a dense facet with a lower interfacial energy because the interfacial energy between solid and liquid changes for variations of crystallographic directions.^[21,25] Therefore, it is seen that during the solidification of alloys, the globularization of alloys with a faceted interface such as Si primary crystals of the ALTHIX 86S alloy can occur due to the higher entropy of the interfacial energy compared to alloys with a nonfaceted interface. This is due to the greater difference in structure and bonding between the solid and liquid phases as compared to metals, which exhibit only very small differences between the two phases. More research on the deformation behavior in the reheating process of eutectic alloys is necessary.

Currently, research, development, and application for thixoforming are limited to a few casting alloys such as A356 and A357 classified into Al-Si-Mg alloy group. However, it is seen that with the increasingly widespread use of thixoforming parts, the development of a tailored alloy for a specific application has to be chosen. Therefore, in this study, the effect of the induction heating conditions of the ALTHIX

86S alloy on globular microstructure, grain growth, and the prevention of coarsening was researched. The ALTHIX 86S alloy contains the composition of Al-6 pct Si-3 pct Cu-0.3 pct Mg and strengthens by age hardening.

In the case of ALTHIX 86S, segregation in which silicon and copper are the principal alloying elements often occurs as a defect in the forming process.^[21,27,28] However, a uniform microstructure without segregation can be obtained in the thixoforming process.

In this study, because a fine and completely melted eutectic Si phase of ALTHIX 86S was obtained, it is expected that thixoforming parts with good mechanical properties will be produced.

X. CONCLUSIONS

To apply the thixoforging and semisolid die casting processes, the optimal coil design of ALTHIX 86S alloys with $d\ 3\ 1\ 5\ 76\ 3\ 70$ (mm) was theoretically proposed and manufactured. The suitability of the coil design was demonstrated by conducting induction-heating experiments. Based on the experiment, the following can be summarized.

1. For the ALTHIX 86S billet with $d\ 3\ 1\ 5\ 76\ 3\ 70$ (mm) (the frequency of the induction heating system: 60 Hz) often used in the thixoforming process, the optimal coil design for induction heating was proposed.
2. This study shows that the larger the billet size, the better the multistep reheating compared with reported results, and the heating time and the capacity of the induction heating system must be increased. We could see that the final holding time of 3 minutes is suitable to secure a globular microstructure.
3. If the reheating holding time of the final step is too short, a globular microstructure cannot be obtained and, if the holding time is too long, because the risks of grain coarsening may be increased. A fine globular microstructure is obtained with a holding time of 3 minutes at the three-step reheating process.

REFERENCES

1. R. Sebus and G. Henneberger: *Proc. 5th Int. Conf. on Semi-Solid Processing of Alloys and Composites*, Golden, CO, June 1998, A.K. Bhasin, J.J. Moore, K.P. Young, and S. Midson, eds., Colorado School of Mines, Golden, CO, 1998, pp. 481-87.
2. F. Matsuura and S. Kitamura: *Proc. 5th Int. Conf. on Semi-Solid Processing of Alloys and Composites*, Golden, CO, June 1998, A.K. Bhasin, J.J. Moore, K.P. Young, and S. Midson, eds., Colorado School of Mines, Golden, CO, 1998, pp. 489-96.
3. S. Midson, V. Rudnev, and R. Gallik: *Proc. 5th Int. Conf. on Semi-Solid Processing of Alloys and Composites*, Golden, CO, June 1998, A.K. Bhasin, J.J. Moore, K.P. Young, and S. Midson, eds., Colorado School of Mines, Golden, CO, 1998, pp. 497-504.
4. V.I. Rudnev, R.L. Cook, D.L. Loveless, and M.R. Black: *Steel Heat Treatment Handbook*, Marcel Dekker Inc., New York, NY, 1997, pp. 794-857.
5. V.I. Rudnev and R. L. Cook: *Forging Mag.*, 1995, Winter, pp. 27-30.

6. V.S. Nemkov, V.B. Demidovich, V.I. Rudnev, and O. Fishman: *Proc. XIIIth Electroheat Congress ELECTROTECH 92*, Montreal, 1992, IEEE and EMC Society, Montreal, 1992, pp. 180-88.
7. V.I. Rudnev and D.L. Loveless: *Industrial Heating*, 1995, Jan., part 1, pp. 29-34.
8. G. Wan, T. Witulski, and G. Hirt: *Int. Conf. on Aluminium Alloys: New Process Technologies*, Marina di Ravenna, June 1993.
9. T. Witulski, U. Morjan, I. Niedick, and G. Hirt: *Proc. 5th Int. Conf. on Semi-Solid Processing of Alloys and Composites*, Golden, CO, June 1998, A.K. Bhasin, J.J. Moore, K.P. Young, and S. Midson, eds., Colorado School of Mines, Golden, CO, 1998, pp. 353-60.
10. M. Garat, S. Blais, C. Pluchon, and W.R. Loue': *Proc. 5th Int. Conf. on Semi-Solid Processing of Alloys and Composites*, Golden, CO, June 1998, A.K. Bhasin, J.J. Moore, K.P. Young, and S. Midson, eds., Colorado School of Mines, Golden, CO, 1998, pp. xvii-xxxi.
11. C. Pluchon, W. Loue' and M. Garat: *Proc. Symp. on Forming Technology of Semi-Solid Metals*, Pusan, Nov. 1997, C.G. Kang, ed., KSTP and KIMM, Pusan National University, Pusan, 1997, pp. 80-95.
12. W. Loue' and M. Garat: *Proc. Symp. on Forming Technology of Semi-Solid Metals*, Pusan, Nov. 1997, C.G. Kang, ed., KSTP and KIMM, Pusan National University, Pusan, 1997, pp. 96-104.
13. M. Garat: *Proc. Symp. on Forming Technology of Semi-Solid Metals*, Pusan, Nov. 1997, C.G. Kang, ed., KSTP and KIMM, Pusan National University, Pusan, 1997, pp. 105-13.
14. C.G. Kang, Y.J. Do, and S.S. Kang: *J. Kor. Soc. Technol. Plasticity*, 1998, vol. 7 (3), pp. 215-24.
15. H.K. Jung and C.G. Kang: *J. Kor. Foundrymen's Soc.*, 1998, vol. 18 (5), pp. 450-61.
16. E.J. Davies: *Conduction and Induction Heating*, Peter Peregrinus Ltd., London, 1990, pp. 100, 164-79, and 202-22.
17. N.R. Stansel: *Induction Heating*, McGraw-Hill, New York, NY, 1949, p. 178.
18. V.I. Rudnev, L.C. Raymond, D.L. Loveless, and M.R. Black: *Induction Heat Treatment*, Marcel Dekker Inc., New York, NY, 1997, pp. 775-911.
19. *Metals Handbook: Properties and Selection: Nonferrous Alloys and Special Purpose Materials*, 10th ed., ASM INTERNATIONAL, Materials Park, OH, 1990, vol. 2, pp. 164-66.
20. C.G. Kang, H.K. Jung, and Y.J. Jung: *Proc. 6th Int. Conf. on Technology of Plasticity (ICTP)*, Nuremberg, Sept. 1999, M. Geiger, ed., VDI and WGP, Friedrich-Alexander-University, Nuremberg, Germany, 1999, in press.
21. C.G. Kang, Y.H. Kim, and H.K. Jung: "Thixoforming Process Development of Aluminum Materials," Technical Report No. NSDM 98K3-0908-01-01-3, Engineering Research Center for Net Shape and Die Manufacturing, Pusan National University, Pusan, 1999.
22. C.G. Kang, H.K. Jung, and N.S. Kim: *Int. J. Mech. Sci.*, 1999, vol. 41(12), pp. 1423-45.
23. I.J. Kim and D.H. Kim: *J. Kor. Foundrymen's Soc.*, 1997, vol. 17(4), pp. 311-18.
24. C.G. Kang and J.Y. Kang: "The Process Development on Thixoforming of Aluminium Materials," Technical Report, No. NSDM 97K3-0908-01-01-3, Engineering Research Center for Net Shape and Die Manufacturing, Pusan National University, Pusan, Feb. 1998.
25. W. Kurz and D.J. Fisher: *Fundamentals of Solidification*, Trans Tech Publications, Aedermannsdorf Switzerland, 1984, pp. 34-43.
26. G. Hirt, R. Cremer, A. Winkelmann, T. Witulski, and M. Zillgen: *J. Mater. Processing Technol.*, 1994, vol. 45, pp. 359-64.
27. C.G. Kang, K.D. Jung, and H.K. Jung: *Proc. 2nd Int. Conf. on Intelligent Processing and Manufacturing of Materials (IPMM)*, Honolulu Hawaii, July 1999, J.A. Meech, M.M. Veiga, M.H. Smith, and S.R. LeClair, eds., West Coast Reproduction Centers, Vancouver, B.C., 1999, pp. 593-99.
28. S. Kouji: *Proc. 175th JSTP Symp. for Semi-Solid Metals Forming*, Tokyo, May 1997, M. Kiuchi, ed., JSTP and JSME, Tokyo University of Technology, Tokyo, 1997, pp. 25-33.